PROGRESSIVE DAMAGE OF RANDOMLY ORIENTED SHORT FIBER REINFORCED COMPOSITES

J. J. Jeong*, H. - J. Chun*, S. H. Byun*, J. H. Byun and M. K. Um****
***School of Mechanical Engineering, Yonsei University, 134 Shinchon-dong, Seodaemun-gu, Seoul 120-749, Korea**
****Korea Institute of Machinery and Materials, 66 Sangnam-Dong, Changwon, Kyungnam 641-010, Korea**

Keywords*: short fiber composites, partial debonding, progressive damage*

Abstract

Recently, short fiber reinforced composites are widely utilized in many structural parts in automobile, infrastructure and electric equipment applications due to their high specific strength, high specific stiffness, long fatigue life and high impact resistance as well as cost effective capability of production. If these parts are exposed to low-velocity impact, significant damages may develop inside the composite parts. These damages may cause reduction of mechanical performances of composite parts. Therefore, predictive analytical or numerical tools are required to evaluate and analyze the integrity of composite parts with impact damages.

In this study, a user-defined material subroutine incorporating damage mechanisms of short fiber reinforced composites was developed adopting and modifying various damage models. Then, the subroutine is implemented into ABAQUS to conduct analysis of short fiber reinforced composites parts. The results were compared with those without considering damage mechanism.

1. Introduction

One of major issues in today's automobile and electric home appliance industries is developing stronger and lighter products. In response to the demands, light weight and high specific strength fiber reinforced composites are being applied extensively. According to the types of fiber, fiber reinforced composites are divided into long fiber reinforced composites and short fiber reinforced composites. Compared to short fiber reinforced composites, long fiber reinforced composites have superior mechanical properties in the fiber direction and usually used for high performance products such as aerospace applications. However, their fabrication processes are complicated and require sophisticated facilities. Also, it is difficult to implement them to mass production processes. On the contrary, the short fiber reinforced composites is inferior to long fiber reinforced composites in mechanical performances, but they can be shaped into variety of forms and is easy to apply to resin injection procedures, thus it is easier to implement them to mass productions. For these reasons, it is reasonable to apply short fiber reinforced composites to some automobile parts and electric home appliance products, in which mass production is essential. For example, metal parts in the automobile such as intake manifolds, junction boxes, HVAC (Heating, Ventilating and Air Conditioning) cases, engine gaskets and various structural parts have been replaced with equivalent stiffness short fiber nylon composites for weight reduction. In mobile phones, emphasizing slimness, traditional magnesium cases are replaced with short fiber reinforced Polyphthalamide resin for efficient mass production.

As short fiber reinforced composite products are being developed actively throughout industries, it is necessary to understand the properties and behaviors of short fiber reinforced composites from the designer's viewpoint. In addition, for the reliability of short fiber reinforced composite products, the integrity of the products under impact conditions must be considered. Unfortunately recent commercial packages do not provide accurate damage process of short fiber reinforced composites. Therefore, predictive analytical or numerical tools are required to evaluate and analyze the integrity of composite parts with impact damages.

In order to understand the behaviors of short fiber reinforced composites under impact loading, understanding of micromechanics and fracture mechanics associated with of short fiber reinforced composites is needed. The short fiber reinforced

composites have the characteristic of heterogeneous materials in which short fibers are arranged disorderly in the random directions on homogeneous matrix. In addition, due to perturbed strain between the fiber and the matrix and interaction effect among fibers, the general elastoplastic theories of homogeneous materials can not be applied as they are. To overcome such difficulties, Ju and Chen [1-3] averaged the whole of the components by applying the concept of mesoscopic representative volume element to short fiber reinforced composite composed of two phases, namely, matrix and inclusion. They proposed an effective constitutive equation that can homogenize the properties of heterogeneous materials. Based on the constitutive equation, Ju and Tseng [4] explained elastoplastic behavior through an effective yield criterion that adopted stress norm averaged as a whole at an arbitrary position inside short fiber reinforced composites. In addition, phenomena appearing in the damage mechanism of short fiber reinforced composites are divided largely into the interfacial debonding between the matrix and fibers, facture of fiber, and fracture of matrix. Particularly, because interfacial debonding among the components brings microcracks inside the composite, it is the most important factor to be considered in fracture mechanism. For a quantitative approach to the degree of interfacial debonding, Ju and Lee [9] predicted elastoplastic behavior in terms of interfacial complete debonding between the matrix and fibers using Weibull's probability distribution function. Zhao and Weng [5, 6] and Ju and Lee [8] also used Weibull's probability distribution function to predict elastoplastic behavior in terms of interfacial partial debonding between the matrix and fibers.

Because the short fiber reinforced composite shows the behavior of a brittle material with a very short plastic zone, it is more efficient to approach the fracture mechanism after interfacial debonding between the matrix and fibers than to use an effective yield criterion and stress norm [10]. In fracture mechanics, behavior after plastic yielding can be expressed using the size of microcracks and the number of microcracks per unit volume. If stress on the material is higher than crack initiation stress, cracks are nucleated inside the material [12] and grow according to energy balance conditions [13] and the growth rate depends on the Rayleigh wave speed proposed by Freund [11].

In this study, in order to produce more accurate results of simulation reflecting behavioral characteristics related to the plasticity and fracture of short fiber reinforced composites, the effects of elastoplastic behavior and fracture process after interfacial debonding between the matrix and fibers are incorporated in the numerical model, and linked to commercial package, ABAQUS.

2. Damage Mechanism of Short Fiber Reinforced Composites

The short fiber reinforced composites are composed of matrix (Phase 0), perfectly bonded fibers (Phase 1), microcracks (Phase 3), and voids (Phase 4) (see Fig. 1 (a)). When short fiber reinforced composites are subject to remote tensile loading (see Fig. 1 (b)), some fibers may experience partial debonding between the matrix and fibers as deformations proceed. As a result, partially debonded fibers (Phase 2) appear newly in short fiber reinforced composite.

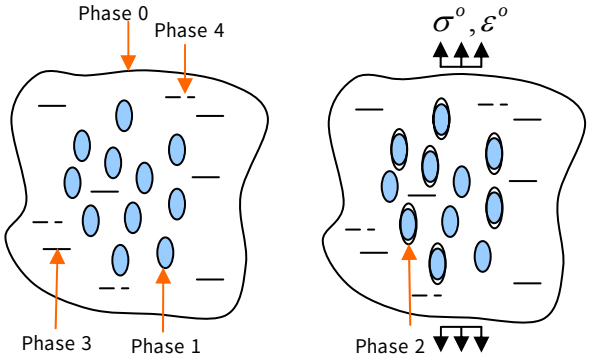

(a) Initial condition (b) Under loading

Fig. 1. Schematic diagrams of short fiber reinforced composite

In order to regard short fiber reinforced composite as an equivalent homogeneous continuum medium, effective Young's modulus E_e and Poisson's ratio ν_e can be derived by applying the concept of the representative volume element representing heterogeneous domains and ensemble averaging of the properties of all heterogeneous domains. Effective stiffness tensor is expressed as their function and it is expressed as

$$C_{ij} = C(E_e, \nu_e) \tag{1}$$

The degree of moduli (E^*, ν^*, G^*) degraded by crack nucleation and crack growth are derived through differential scheme estimate.

$$\frac{E^*}{E_e}=\left(\frac{\nu^*}{\nu_e}\right)^{10/9}\left(\frac{3-\nu_e}{3-\nu^*}\right)^{1/9},$$
$$\frac{G^*}{G_e}=\frac{1+\nu_e E^*}{1+\nu^* E_e}, \qquad (2)$$
$$\omega=\frac{5}{8}\ln\frac{\nu_e}{\nu^*}+\frac{15}{64}\ln\frac{1-\nu^*}{1-\nu_e}+\frac{45}{128}\ln\frac{1+\nu^*}{1+\nu_e}+\frac{5}{128}\ln\frac{3-\nu^*}{3-\nu_e}$$
$$=N\bar{c}^3$$

where ω, N and $\bar{c}$ are crack density, number of microcracks per unit volume and mean crack radius, respectively. Degradation stiffness tensor is a function of degradation Young's modulus E^* and Poisson's ratio ν^* derived from Eq. (2), and it is as

$$C_{ij} = C(E^*, \nu^*) \qquad (3)$$

Damage mechanism of short fiber reinforced composites has 3-processes, interfacial debonding of fibers, the crack nucleation and crack growth.

First, the evolutionary interfacial debonding between matrix and perfectly boned fibers occurs under increasing loading or deformations, and debonded fibers can be regarded as partially debonded fibers. Volume fraction ϕ_2 of the partially debonded fibers assume to be controlled by the hydrostatic stress $(\bar{\sigma}_m)_1$ of the fibers, and criterion for debonding fibers can be expressed using Weibull's statistical function $P_d[(\bar{\sigma}_m)_1]$ [1] as

$$\phi_2 = \phi P_d[(\bar{\sigma}_m)_1] = \phi\left\{1-\exp\left[-\left(\frac{(\bar{\sigma}_m)_1}{S_O}\right)^M\right]\right\} \qquad (4)$$

where, S_0 and M are scale and shape parameter of Weibull's statistical function, respectively, and ϕ is the initial volume fraction of fibers.

Second, the criterion of microcrack nucleation can be expressed as an exponential relation using initial stress σ_{no} for the nucleation of micro cracks and it is give as

$$\begin{cases} \dot{N}=0 & when\ \ \sigma \le \sigma_{no} \\ \dot{N}=\dot{N}_0\cdot\exp\left[\dfrac{\sigma-\sigma_{no}}{\sigma_1}\right] & when\ \ \sigma \rangle\ \sigma_{no} \end{cases} \qquad (5)$$

where $\dot{N}$ is the number of microcracks per unit volume and σ_1 is an experimentally determined parameter. It is assumed that the applied stress is defined as $\sigma = [(\sigma_{11})+(\sigma_{22})+(\sigma_{33})]/3$. For the backward Euler method, $\dot{N}$ can be written in an incremental form as

$$N_{n+1} = N_n + \Delta t_{n+1}\dot{N}_o\cdot\exp\left[\frac{(\sigma)_{n+1}-\sigma_{no}}{\sigma_1}\right] \qquad (6)$$

where N_{n+1} is the number of microcracks per unit volume at time $t = t_{n+1}$. If the volume fraction of partially debonded fibers reaches the maximum value and if current stress is satisfied with crack nucleation rate relationship of Eq. (5), crack nucleation increases in short fiber reinforced composites [4].

Lastly, the crack growth criterion of microcracks can be derived by considering energy balance around the microcracks and damage surfaces $F(p,q,\bar{c})$. It can be expressed with pressure p, deviatoric stress q, and mean crack radius $\bar{c}$ of microcracks.

It is expressed in tension (p<0) as

$$F^n(p,q,\bar{c}) = q^2 + \frac{45}{4(5-\nu_0)}\left[(2-\nu_0)p^2 - \frac{2K}{\bar{c}}\right] \qquad (7)$$

and in compression (p>0) as

$$F^t(p,q,\bar{c}) = q^2 - \frac{45}{2(3-2\mu_f^{\,2})}\left[\left(\mu_f p+\sigma_0+\sqrt{\frac{\pi K}{\bar{c}}}\nu_0\right)+\frac{K}{\bar{c}}\right] \qquad (8)$$

where K is defined by plane strain facture toughness and shear modulus [5]. σ_0 is cohesive stress and μ_f is the coefficient of friction. If $F(p,q,\bar{c})>0$, cracks will grow until the rate of crack growth, $\dot{\bar{c}}$, satisfies the requirement $F(p,q,\bar{c})\le 0$. For the backward Euler method, $\dot{\bar{c}}$ can be written in an incremental form as

$$\bar{c}_{n+1} = \bar{c}_n + \Delta t_{n+1}\beta\sqrt{\frac{E^*}{\rho^*}}tanh(d_s) \qquad (9)$$

where $\bar{c}_{n+1}$ is the mean radius of microcrack at time $t = t_{n+1}$, β is a scaling factor for crack speed and is assumed to be a constant. d_s is the measure of the distance the amount by which the state of the stress exceeds the damage surface.

The basic assumption of the fracture mechanics based damage model is that the damaged state of a solid can be described by the number of microcracks per unit volume N and the mean radius $\bar{c}$ of microcracks. Using Eqs. (1) - (9), the constitutive relation for short fiber reinforced composites with statistically uniformly distributed microcracks can be expressed as

$$\sigma = C(\bar{c}, N):\varepsilon \qquad (10)$$

where σ is the macroscopic stress, C is the overall stiffness tensor, ε is the macroscopic strain, and " : " denotes the tensor contraction. The rate form of Eq. (10) can be expressed as

$$\dot{\sigma} = \frac{\partial \mathrm{C}}{\partial N}\dot{N} : \varepsilon + \frac{\partial \mathrm{C}}{\partial \bar{c}}\dot{\bar{c}} : \varepsilon + \mathrm{C} : \dot{\varepsilon} \qquad (11)$$

The numerical integration algorithm must be employed to integrate the rate equations in Eq. (11). Consequently, the overall macroscopic stress can be written as [14]

$$\begin{aligned}\sigma_{n+1} = \sigma_n + \mathrm{C} : \Delta\varepsilon_{n+1} + \frac{\partial \mathrm{C}}{\partial \bar{c}}\Delta\bar{c}_{n+1} : \varepsilon_n + \frac{\partial \mathrm{C}}{\partial \bar{c}}\Delta\bar{c}_{n+1} : \Delta\varepsilon_{n+1} \\ + \frac{\partial \mathrm{C}}{\partial N}\Delta N_{n+1} : \varepsilon_n + \frac{\partial \mathrm{C}}{\partial N}\Delta N : \Delta\varepsilon_{n+1}\end{aligned} \qquad (12)$$

where the subscript n denotes the nth integration time step.

3. Numerical Damage Model

3.1 Damage Model for Short Fiber Reinforced Composites

Because the short fiber reinforced composites show the behaviors of brittle materials, it is more efficient to approach the damage process after interfacial debonding between the matrix and fibers than to use an effective yield criterion and stress norm.

In the present study, the fracture process of short fiber reinforced composites is composed of an algorithm that crack growth proceeds when the state of interfacial debonding of fibers is confirmed and the volume fraction of partially debonded fibers ϕ_2, which is increased by interfacial debonding, reaches the maximum level. Then, microcracks are nucleated. These assumptions are based on that the interfacial debonding between the matrix and the fibers tends to have partial debonding. It can transmit internal stress into the matrix through the bonded portion and, as a result, cracks do not grow until volume fraction ϕ_2 in Phase 2 reaches the maximum level. In addition, the initial mean radius of microcracks $\bar{c}_0$ and the number of initial microcracks per unit volume N_0 to be considered in the damage process after interfacial debonding are considered as the size and number of microcracks occurring by the interfacial partial debonding between the matrix and fibers. The flow diagram of damage analysis procedure is shown in Fig. 2.

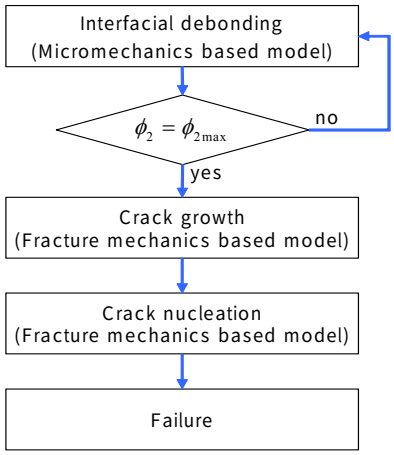

Fig. 2. Flow diagram for damage analysis procedure

3.2 Equivalent Mean Crack Radius of Partially Deboned Fiber

As mentioned in Section 3.1, the initial mean radius of microcracks $\bar{c}_0$ to be considered after interfacial debonding between the matrix and fibers is chosen based on the state of fibers in the matrix. As in Fig. 3, interfacially debonded fiber has microcracks as many as those in the the debonded domain, and the volume V_C is given as

$$V_C = \frac{4}{3}\pi(\alpha' a_2^3 - \alpha a_2^3) = \frac{4}{3}\pi a_2^3 \alpha(\beta_{CF} - 1) \qquad (13)$$

where $\alpha' = a_1'/a_2$ is aspect ratio (ratio of length to diameter) of spheroidal microcrack, $\alpha = a_1/a_2$ is aspect ratio of spheroidal fiber, and β_{CF} is ratio of α' to α. Using Eq. (13), equivalent mean crack radius $\bar{c}_0$ of partially debonded fiber can be calculated as

$$\bar{c}_0 = \sqrt[3]{a_2^3 \alpha(\beta_{CF} - 1)} \qquad (14)$$

Likewise, the number of initial microcracks per unit volume N_0 to be considered after interfacial debonding between the matrix and fibers is related to fiber volume fraction ϕ_2 in Phase 2 where interfacial debonding takes place. Then, the relationship is established as

$$\phi_2 = \frac{V_{d-fiber} \times n}{V_{composite}} = V_{d-fiber} \times N_0 \times \beta_{NF} \qquad (15)$$

where $V_{d-fiber}$ and $V_{composite}$ denote the volume of debonded fiber and the volume of short fiber reinforced composites, respectively. β_{NF} is a scaling factor for the number of microcracks. Consequently,

the number of initial microcracks per unit volume N_0 can be calculated as

$$N_0 = \frac{3\phi_2}{4\pi\alpha a_2^3}\beta_{NF} \tag{16}$$

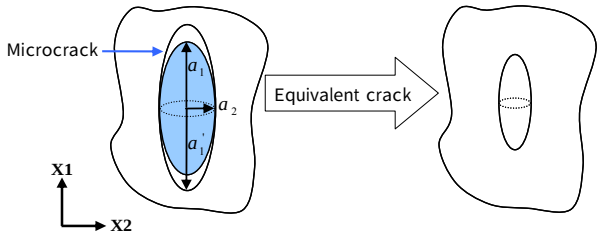

Fig. 3. Equivalent crack size

3.3 Differential Coefficients for Damage Model

As expressed in Eq. 12., in order to derive a constitutive equation for the damage model of short fiber reinforced composites, stiffness matrix $C_{ij}(E^*,\nu^*)$ in Eq. (3), which is a function of degradation Young's modulus E^* and Poisson's ratio ν^*, should be expressed in the form of a derived function of mean radius of microcracks $\bar{c}$ and the number of microcracks per unit volume N.

$$\frac{\partial C_{ij}(E^*,\nu^*)}{\partial \bar{c}} = \frac{\partial C_{ij}(E^*,\nu^*)}{\partial E^*}\cdot\frac{\partial E^*}{\partial \bar{c}} + \frac{\partial C_{ij}(E^*,\nu^*)}{\partial \nu^*}\cdot\frac{\partial \nu^*}{\partial \bar{c}} \tag{17}$$

$$\frac{\partial C_{ij}(E^*,\nu^*)}{\partial N} = \frac{\partial C_{ij}(E^*,\nu^*)}{\partial E^*}\cdot\frac{\partial E^*}{\partial N} + \frac{\partial C_{ij}(E^*,\nu^*)}{\partial \nu^*}\cdot\frac{\partial \nu^*}{\partial N} \tag{18}$$

Using Eq. (2), the differential coefficients of Eqs. (17) and (18) are derived as

$$\frac{\partial E^*}{\partial \bar{c}} = \frac{\partial E^*}{\partial \nu^*}\cdot\frac{\partial \nu^*}{\partial \omega}\cdot\frac{\partial \omega}{\partial \bar{c}},\ \frac{\partial E^*}{\partial N} = \frac{\partial E^*}{\partial \nu^*}\cdot\frac{\partial \nu^*}{\partial \omega}\cdot\frac{\partial \omega}{\partial N} \tag{19}$$

$$\frac{\partial \nu^*}{\partial \bar{c}} = \frac{\partial \nu^*}{\partial \omega}\cdot\frac{\partial \omega}{\partial \bar{c}},\ \frac{\partial \nu^*}{\partial N} = \frac{\partial \nu^*}{\partial \omega}\cdot\frac{\partial \omega}{\partial N} \tag{20}$$

3.4 Finite Element Model

A user-defined material subroutine with damage constitutive model composed of the partial debonding of fiber, crack nucleation and crack growth, is implemented into ABAQUS. The subroutine is written in FORTRAN language. The model is composed of the stage of deriving an effective stiffness matrix using input material properties, the stage of evaluating the evolutionary interfacial debonding between the matrix and perfectly boned fibers, the stage of deriving a degradation stiffness matrix caused by the occurrence of microcracks, the stage of confirming the stability of microcracks and calculating the size of growing cracks, and the stage of confirming the occurrence of microcracks and deriving the number of increased cracks.

3.5 Numerical Simulation for Short Fiber Reinforced Composites

The simulations were performed under different conditions by linking the user defined material subroutines (UMAT, VUMAT) formulated in Section 3.4 to ABAQUS 6.5. First, subroutine UMAT was applied in order to understand the overall damage behavior of short fiber reinforced composite. The simulations shown in Figs. 4 ~ 6 were performed to understand the influence of fiber parameters such as fiber volume fraction ϕ and aspect ratio of fiber and strain rate $\dot{\varepsilon}$. In addition, subroutine VUMAT was applied in order to test the effectiveness of damage behavior caused by crushing and simulation was performed for a rectangular tube crushing at high speed as in Fig. 6 in order to understand fracture observed in crushing.

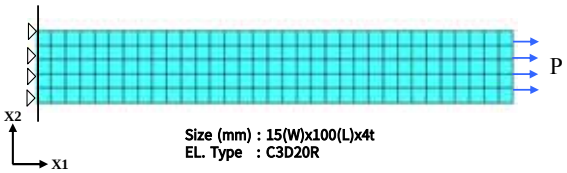

Fig. 4. Tensile stress simulation condition

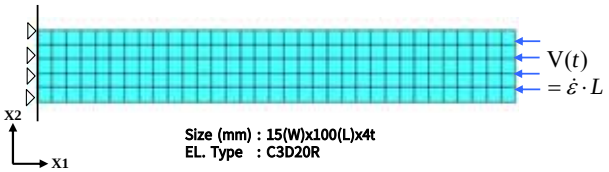

Fig. 5. Compressive stress simulation condition

The material properties of short fiber reinforced composite used in this simulation are adopted from [10] (see Table 1). Theses values are chosen from the literatures and do not correspond to a specific material.

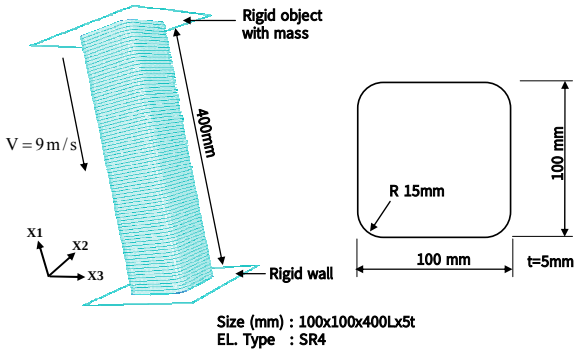

Fig. 6. Crushing simulation condition and geometry

Table 1. Properties of short fiber reinforced composite for numerical simulation

Properties of short fiber reinforced composite	Value
Young's modulus of matrix, E_m, MPa	3e3
Young's modulus of fiber, E_f, MPa	72e3
Poisson's ratio of matrix, ν_m	0.35
Poisson's ratio of matrix, ν_f	0.17
Parameter of Weibull's statistics function, S_0, MPa	163.5
Parameter of Weibull's statistics function, M	4.0
Aspect ratio of spheroid fiber, α	5.0
Density of composite, ρ, $tonne/mm^3$	1.4e-9
Volume fraction of fiber, ϕ	0.3
Coefficient of friction, μ_f	1.0e10
Threshold stress for the nucleation of microcracks, σ_{no}, MPa	1e4
Cohesive stress, σ_0, MPa	0
Scaling factor of crack speed, β	1e-6
Experimental stress for crack nucleation, σ_1, MPa	2e3
Plane strain fracture toughness, K_{IC}, Pa.m	10

4. Results of Simulation

4.1 Equivalent Mean Crack Radius of Partially Debonded Fiber

Fig. 7 shows the result of simulated stress-strain behavior when initial volume fraction ϕ was applied to short fiber reinforced composites. Here, ϕ was applied for 0.1, 0.3 and 0.5. With the increase of ϕ, the stiffness of short fiber reinforced composite increased but its strain of yield decreased. Fig. 8 shows change in volume fraction ϕ_2 of partially debonded fiber. According to the figure, when ϕ is large, ϕ_2 reached the maximum volume fraction at low strain. Fig. 9 shows change in the mean radius of microcracks $\bar{c}$ as a function of ϕ. In the figure, when ϕ is low, the strain of initial crack growth is somewhat slower than that in fibers of different volume fractions but crack growth is faster when the strain exceeds a specific level. This is an important characteristic explaining the reinforcing function of short fiber. Fig. 10 shows the effect of partially debonded fiber on the elastic behavior with the increase of strain. If partially debonded fibers are not considered, stiffness as well as yield strain increases. Accordingly, if the degradation caused by partially debonded fiber is not considered, the properties of short fiber composites cannot be predicted accurately.

The relationship between the aspect ratio of fiber α and stress-strain behavior is shown in Fig. 11. Here, simulation was performed with varying α from 5 to 10 and 20 while fixing ϕ at 0.3. According to the results, with the increase of α, stiffness was improved but yield strength decreased. This characteristic can be explained with the results in Fig. 12 that predicted the change in $\bar{c}$ according to α. This is because, with the increase of α, the initial mean radius of microcracks $\bar{c}_0$ caused by partially debonded fiber becomes relatively large and as a result crack growth causing the degradation of stiffness takes place at lower stress. Accordingly, it is very important to find the optimal condition of α.

The effectiveness of a damage model formulated in this study was examined by comparing it with experimental data for overall uniaxial tensile response of short fiber reinforced composite [15], and the results are presented in Fig. 13. The behavior was similar to the prediction model. The properties of short fiber composite applied in this research are as in Table 2, and unmentioned properties are the same as Table 1.

The predicted compressive behaviors while changing strain rate $\dot{\varepsilon}$ from 0.1/s to 0.3/s and 0.5/s, are presented in Fig. 14. When $\dot{\varepsilon}$ was low, damage proceeded at low strain and softening after they reached the ultimate strength were also observed at low strain before fracture. This can be explained with Fig. 15 that predicted change in the mean radius of microcracks $\bar{c}$ is dependent on $\dot{\varepsilon}$. That is, as shown by the results, it is predicted that, when ε=0.05, $\bar{c}$ at $\dot{\varepsilon}$=0.1/s is 2.5 times larger than that at $\dot{\varepsilon}$ =0.5/s. As in Fig. 16 and Fig. 17, Young's modulus E^* and Poisson's ratio ν^* decreased from the moment that $\bar{c}$ began to increase. In this way, crack growth is a major cause of the degradation of short fiber reinforced composite properties. Fig. 18 shows the predicted distance d_s of damage surface, which is a criterion for determining crack growth.

The strain from which d_s begins to become larger than 0 is coincident with the strain from which cracks begin to grow.

The initial mean radius of microcracks $\bar{c}_0$ and number of initial microcracks per unit volume N_0 observed in the interfacial debonding of fiber were predicted to be 0.0172mm and 97.615 (ea/mm3), respectively, when ϕ=0.3 and α=5.

In order to understand phenomena observed in actual impact conditions, a simulation was performed and the result is presented the results in Fig. 19. It was predicted that major fracture and strain take place on the front of the tube.

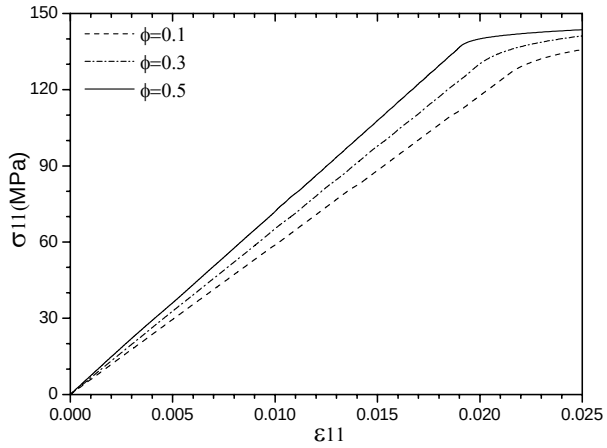

Fig. 7. Predicted tensile stress vs. strain for fiber volume fraction ϕ of 0.1, 0.3, 0.

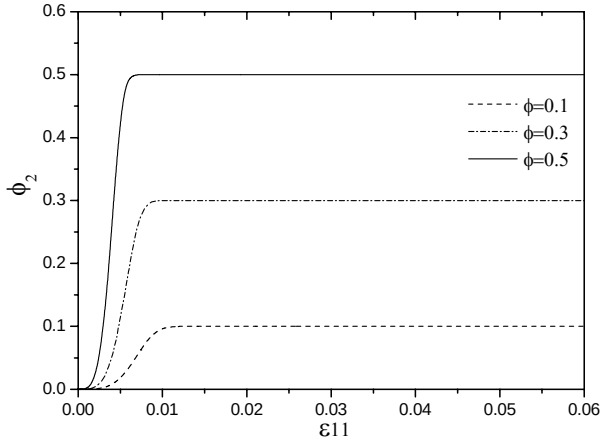

Fig. 8. Predicted evolution of volume fraction ϕ_2 for partially debonded fiber vs. strain for fiber volume fraction ϕ of 0.1, 0.3, 0.5

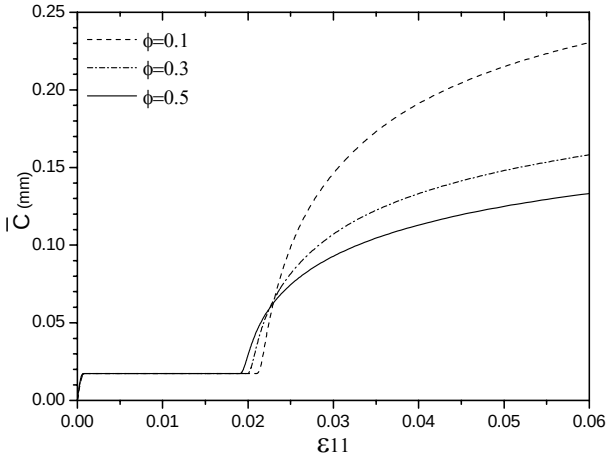

Fig. 9. Predicted evolutions of mean crack size $\bar{c}$ vs. strain for fiber volume fraction ϕ of 0.1, 0.3, 0.5

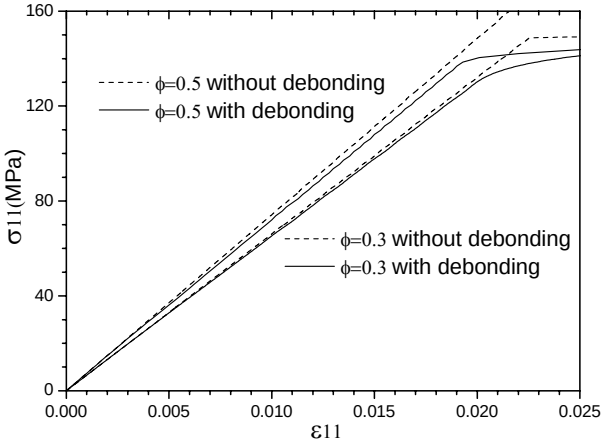

Fig. 10. Effect of partial debonding on the elastic behavior

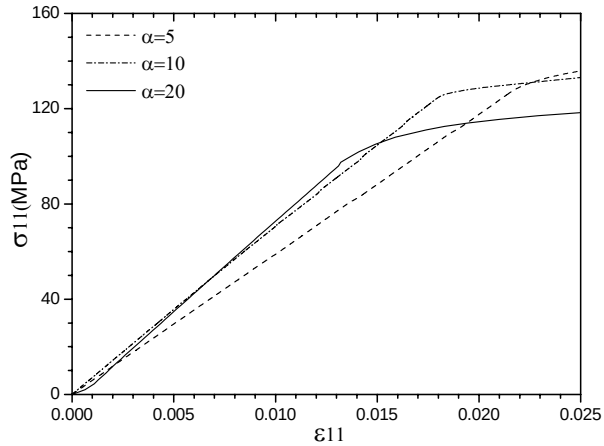

Fig. 11. Predicted tensile stress vs. strain for fiber aspect ratio α of 5, 10, 20

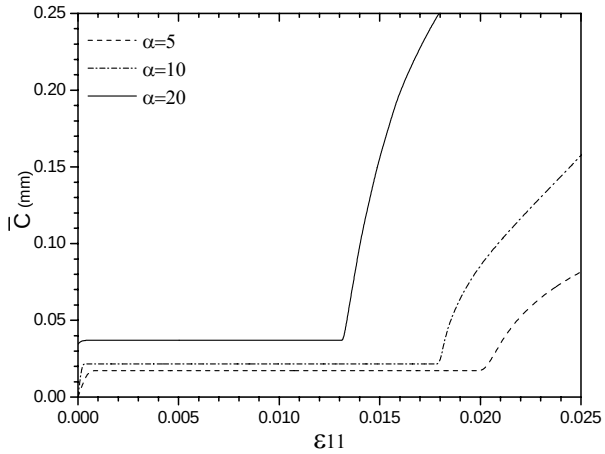

Fig. 12. Predicted evolutions of mean crack size $\bar{c}$ vs. strain for fiber aspect ratio α of 5, 10, 20

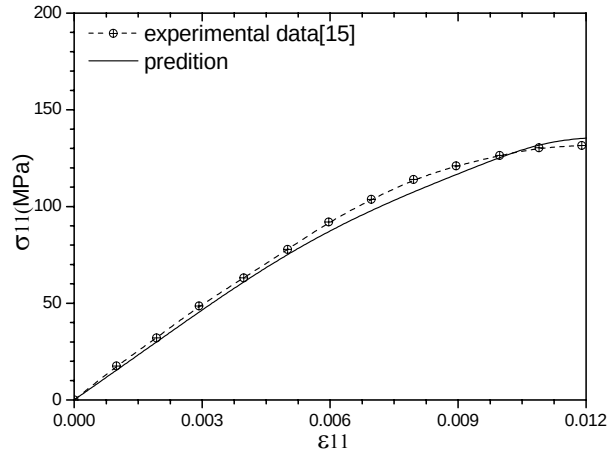

Fig. 13. Comparison between the present prediction and experimental data [15]

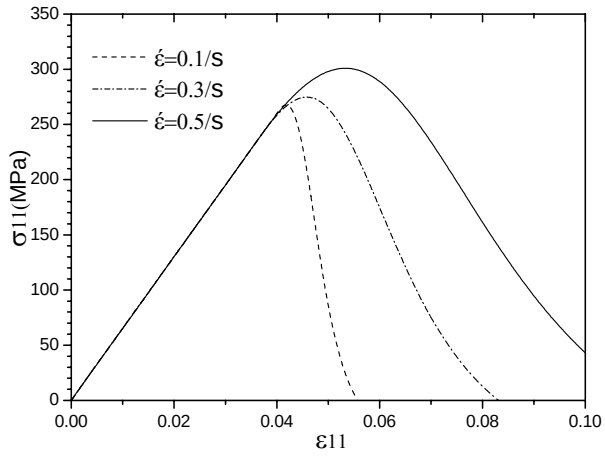

Fig. 14. Predicted compressive stress vs. strain for strain rate $\dot{\varepsilon}$ of 0.1/s, 0.3/s, 0.5/s

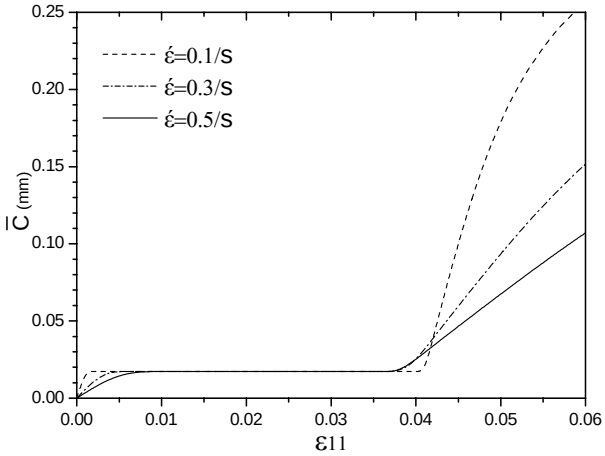

Fig. 15. Predicted evolutions of mean crack radius $\bar{c}$ vs. strain for strain rate $\dot{\varepsilon}$ of 0.1/s, 0.3/s, 0.5/s

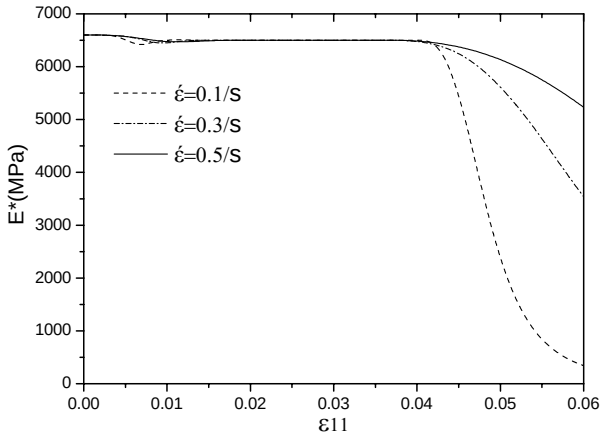

Fig. 16. Predicted effective Young's modulus E^* vs. strain for strain rate $\dot{\varepsilon}$ of 0.1/s, 0.3/s, 0.5/s

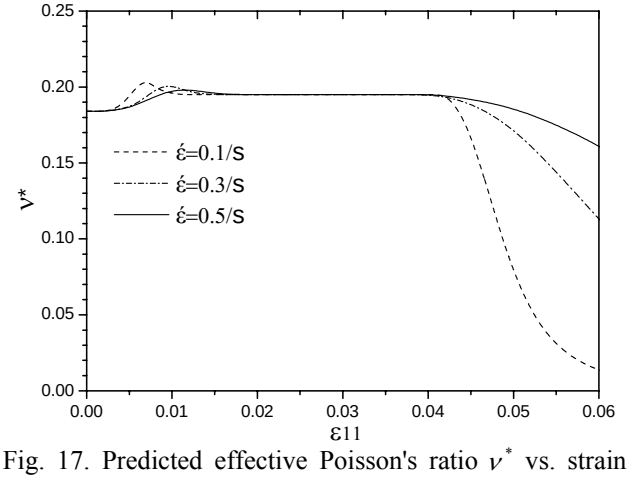

Fig. 17. Predicted effective Poisson's ratio ν^* vs. strain for strain rate $\dot{\varepsilon}$ of 0.1/s, 0.3/s, 0.5/s

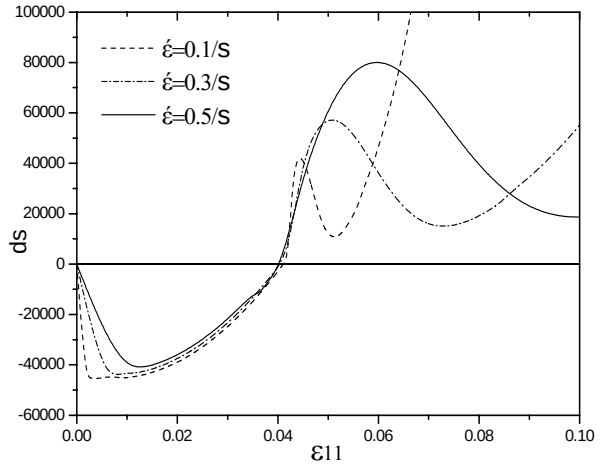

Fig. 18. The predicted distance from damage surface vs. strain for strain rate $\dot{\varepsilon}$ of 0.1/s, 0.3/s, 0.5/s

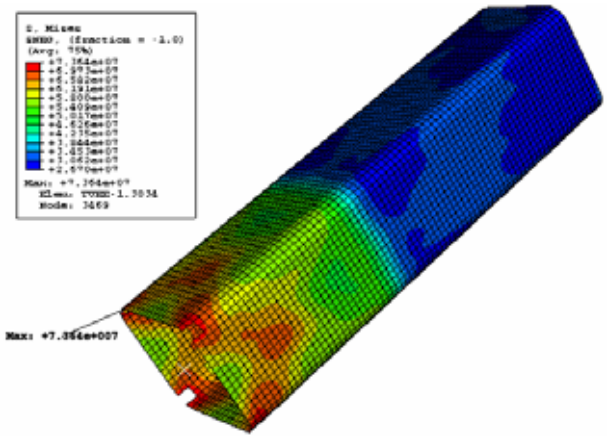

Fig. 19. Result visualization for isometric view (stress unit = Pa)

Table 2. Properties of short fiber reinforced composites for comparison with experimental data [15, 7]

Properties of short fiber reinforced composite	Value
Parameter of Weibull's statistics function, S_0, MPa	600
Volume fraction of fiber, ϕ	0.5
Aspect ratio of spheroid fiber, α	19.25

5. Conclusions

In the present study, the fracture process of short fiber reinforced composites was predicted by a numerical analysis method. A theoretical damage model was formulated using user-defined material subroutines (UMAT, VUMAT) of ABAQUS, and it was linked to the analysis procedure of ABAQUS in order to understand impact damage behavior. From this study, it is found that it is effective to predict elastoplastic behavior of short fiber reinforced composite with a short plastic area using the size of microcracks occurring in interfacial debonding and the number of microcracks per unit volume. Using these findings, a constitutive equation is formulated more easily and effectively than using effective yield functions and stress norm.

In addition, it was found that the mechanical properties of short fiber reinforced composites are heavily affected by the volume fraction and aspect ratio of fiber, and that partially debonded fiber appearing newly in the behavioral process enables the effective prediction of stiffness and plastic strain and determines the size and number of initial cracks, so it must be considered in the damage model. In addition, impact simulation showed that short fiber reinforced composites are very sensitive to strain rate, namely, impact velocity and this suggests that it is most vulnerable to low-velocity impact.

Acknowledgment

This research was supported by a grant from the Center for Advanced Materials Processing (CAMP) of the 21st Century Frontier R&D Program funded by the Ministry of Science and Technology, Republic of Korea.

References

[1] Ju J. W. and Chen T. M. “Micromechanics and effective elastoplastic behavior of two-phase metal-matrix composites”. *J. Engrg. Mat. Technol.*, Vol. 116, pp 310-318, 1994.

[2] Ju J. W. and Chen T. M. “Micromechanics and effective moduli of elastic composites containing randomly dispersed ellipsoidal inhomogeneities”. *Acta Mechanica*, Vol. 103, pp 103-121, 1994.

[3] Ju J. W. and Chen T. M. “Effective elastic moduli of two-phase composites containing randomly dispersed spherical inhomogeneities”. *Acta Mechanica*, Vol. 103, pp 123–144, 1994.

[4] Ju J. W. and Tseng K. H. “Effective elastoplastic behavior of two-phase ductile matrix composites : a micromechanical framework”. *Internat. J. Solids Structures*, Vol. 33, pp 4267-4291, 1996.

[5] Zhao Y. H. and Weng G. J. “Plasticity of a two-phase composite with partially debonded inclusions”. *Internat. J. Plasticity*, Vol. 12, pp 781-804, 1996.

[6] Zhao Y. H. and Weng G. J. “Transversely isotropic moduli of two partially deboned composites”. *Internat. J. Solids Structures*, Vol. 34, pp 93-507, 1997.

[7] Lee H. K. and Simunovic S. “Modeling of progressive damage in aligned and randomly oriented

discontinuous fiber polymer matrix composites" *Composites : Part B*, Vol. 31, pp 77-86, 2000.

[8] Ju J. W. and Lee H. K. "A micromechanical damage model for effective elastoplastic behavior of partially debonded ductile matrix composites". *Internat. J. Solids Structures*, Vol. 38, pp 6307-6332, 2001.

[9] Ju J. W. and Lee H. K. "A micromechanical damage model for effective elastoplastic behavior of ductile matrix composites considering evolutionary complete particle debonding". *Comput. Methods Appl. Mech. Engrg*., Vol. 183, pp 201-222, 2000.

[10] Lee H. K., Simunovic S. and Shin D. K. "A computational approach for prediction of the damage evolution and crushing behavior of chopped random fiber composites". *Comput. Mater. Sci*., Vol. 29, pp 459–474, 2004.

[11] Addessio F. L. and Johnson J. N. "A constitutive model for the dynamic response of brittle materials" *J. Appl. Phys*., Vol. 67, pp 3275–3286, 1990.

[12] Curran D. R., Shockey D. A. and Seaman L. "Dynamic fracture criteria for a polycarbonate". *J. Appl. Phys*., Vol. 44, pp 4025–4038, 1973.

[13] Hashin Z. "The differential scheme and its application to cracked materials". *J. Mech. Phys. Solids*, Vol. 36, pp 719–734, 1988.

[14] Lee H. K., Simunovic S. and . Shin D. K. "Prediction of crack evolution and effective elastic behavior of damage-tolerant brittle composites". *Comput. Methods Appl. Mech. Engrg*. Vol. 196, pp. 118-133, 2006.

[15] Meraghni F. and Benzeggagh M.L. "Micromechanical modeling of matrix degradation in randomly discontinuous-fibre composites". *Compos. Sci. Technol*., Vol. 55, pp 171–186, 1995. .